SIMULTANEOUS DFT AND IDFT THROUGH WIDELY LINEAR CLMS

Xing Zhang[1], Bruno Scalzo Dees[2], Chunguo Li[1], Yili Xia[1], Luxi Yang[1], and Danilo P. Mandic[2]

[1]School of Information Science and Engineering, Southeast University, Nanjing 210096, P. R. China
[2]Department of Electrical and Electronic Engineering, Imperial College London, London SW7 2BT, UK
Emails: {xingzhang, chunguoli, yili_xia, lxyang}@seu.edu.cn, {bs1912, d.mandic}@imperial.ac.uk

ABSTRACT

Complex least mean square (CLMS) based adaptive computation of discrete orthogonal transforms has been extensively investigated in the literature. However, all of these results provide only a means for the calculation of either forward orthogonal transforms or their inverse orthogonal transforms, separately. In this work, a way to simultaneously calculate the discrete Fourier transform (DFT) and the inverse DFT (IDFT) is established via the widely linear (WL) signal processing framework. We show that by appropriately selecting the input vector and adaptation speed of the widely linear complex least mean square (WL-CLMS), the resulting spectrum analyzer is capable of simultaneously performing DFT and IDFT of the signal to be Fourier analyzed in both the block-based and online manners.

Index Terms— DFT, inverse DFT (IDFT), widely linear CLMS, recursive DFT and IDFT spectrum analyzer

1. INTRODUCTION

It is well-known that the classic Fourier coefficients of a signal representation can be obtained by the best least squares fitting of a finite number of sines and cosines. In this sense, the mapping of a signal into its Fourier components can be implemented recursively by virtue of the complex least mean square (CLMS) adaptive filter. This is achieved by choosing harmonic series with quadrature phase terms as the filter input and the signal to be Fourier analyzed as the desired output. This basic idea was first proposed by Widrow *et al.* in [1], whereby both the block-based DFT and its recursive counterpart were computed through a CLMS spectrum analyzer. This made it possible to achieve online DFT computation in a sliding window manner, that is, for streaming data. Based on these findings, more research efforts in this direction include a generalized LMS framework to compute other orthogonal transforms like discrete Hartley transform [2], discrete Walsh transform [3] and discrete cosine/sine analyzer [4], together with their two-dimensional extensions [5–7]. All in all, the CLMS algorithm provides an alternative way to perform various orthogonal transforms and its parallel and adaptive processing nature facilitates VLSI implementation and roundoff error elimination in these orthogonal transforms [1, 8].

However, LMS-based spectrum analyzers only provide a means for the separate calculation of forward orthogonal transforms or their inverses [2–11]. This is a direct consequence of a strictly linear estimation framework which is inherent to traditional adaptive filters in the complex domain, where the second order circularity (properness) assumption is imposed on both the desired and input signals [12]. The signal properness refers to the situation where the real and imaginary components of complex-valued random signals are both uncorrelated and with equal powers, making complex-valued random signals behave like real-valued ones in the sense that their second order statistics is fully described by the standard covariance matrix. This simplifies the complex-valued statistical analysis in many aspects. However, recent results in the so-called *augmented complex statistics* show that in order to fully explore all the available second order information in general complex-valued signals, another second order moment, called the complementary covariance matrix, should also be taken into account, alongside the conventional covariance matrix, especially for improper data [13–16]. This has been achieved through the widely linear (WL) estimation framework which incorporates both the original signals themselves and their complex conjugates [17]. A well-known example in adaptive filter design is the development of WL-CLMS, which has provided modelling advantages over its strictly linear CLMS counterpart in numerous applications in signal processing, communications, power systems, and renewable energy [18–22].

In this paper, intrinsic relations between the WL-CLMS and both the DFT and IDFT operations are investigated. We show that by appropriately selecting the input vector and adaptation speed, the weight coefficients of the proposed WL-CLMS spectrum analyzer provide a means for the simultaneous computation of DFT and IDFT of a complex-valued signal. More specifically, N equally spaced complex phasors and their complex conjugates are weighted by the WL-CLMS to generate a reconstructed signal. These weight vectors are then adapted to provide a best least squares fit between the reconstructed signal and the signal to be analyzed. In this way, the standard and conjugate weights within the augment-

This work was partially supported by the National Science Foundation of China under Grants 61771124 and 61671144.

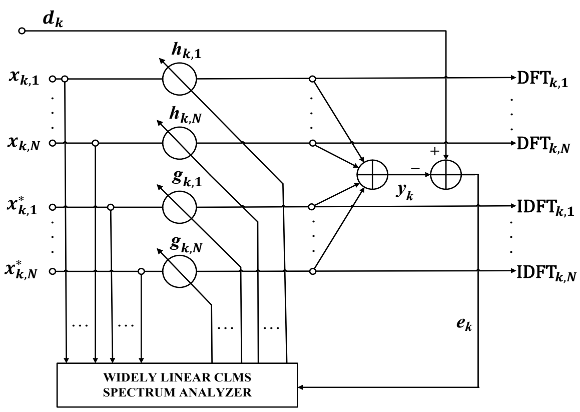

Fig. 1. The proposed WL-CLMS spectrum analyzer.

ed weight vector of the WL-CLMS correspond respectively to the N-DFT and N-IDFT coefficients after N iterations.

2. BLOCK-BASED DFT AND IDFT COMPUTATION BY USING THE WL-CLMS SPECTRUM ANALYZER

The block diagram of the proposed widely linear CLMS spectrum analyzer, used to calculate the N-DFT and N-IDFT operations simultaneously, is shown in Fig. 1. The signal to be Fourier analyzed, i.e., d_k, refers to the desired output of the adaptive filter at the time instant k. The input to the WL-CLMS filter is the complex phasor vector, $\mathbf{x}_k$, and its complex conjugate, $\mathbf{x}_k^*$, respectively given by

$$\mathbf{x}_k = \frac{1}{\sqrt{N}}\left[1, e^{i2\pi k/N}, \ldots, e^{i2\pi(N-1)k/N}\right]^T, \quad (1)$$

$$\mathbf{x}_k^* = \frac{1}{\sqrt{N}}\left[1, e^{-i2\pi k/N}, \ldots, e^{-i2\pi(N-1)k/N}\right]^T, \quad (2)$$

where $(\cdot)^T$ denotes the transpose, $(\cdot)^*$ denotes the complex conjugate, and $i = \sqrt{-1}$. The scaling factor $1/\sqrt{N}$ is introduced for convenience in DFT and IDFT calculations. Both the $N \times 1$ conjugate weight vector $\mathbf{g}_k = [g_{k,1}, g_{k,2}, \ldots, g_{k,N}]^T$ and the $N \times 1$ standard weight vector $\mathbf{h}_k = [h_{k,1}, h_{k,2}, \ldots, h_{k,N}]^T$ are updated in accordance with the WL-CLMS as [14, 19, 20]

$$\mathbf{g}_{k+1} = \mathbf{g}_k + \mu e_k \mathbf{x}_k, \quad (3)$$

$$\mathbf{h}_{k+1} = \mathbf{h}_k + \mu e_k \mathbf{x}_k^*, \quad (4)$$

where $\mu \in \mathbb{R}^+$ is the step-size and the error, e_k, is defined as

$$e_k = d_k - \mathbf{x}_k^T \mathbf{h}_k - \mathbf{x}_k^H \mathbf{g}_k. \quad (5)$$

Substituting (5) back into the weight update processes in (3) and (4) yields

$$\begin{aligned}\mathbf{g}_{k+1} &= \mathbf{g}_k + \mu \mathbf{x}_k\left(d_k - \mathbf{x}_k^T \mathbf{h}_k - \mathbf{x}_k^H \mathbf{g}_k\right)\\ &= \left(\mathbf{I} - \mu \mathbf{x}_k \mathbf{x}_k^H\right)\mathbf{g}_k - \mu \mathbf{x}_k \mathbf{x}_k^T \mathbf{h}_k + \mu d_k \mathbf{x}_k, \quad (6)\end{aligned}$$

$$\mathbf{h}_{k+1} = \left(\mathbf{I} - \mu \mathbf{x}_k^* \mathbf{x}_k^T\right)\mathbf{h}_k - \mu \mathbf{x}_k^* \mathbf{x}_k^H \mathbf{g}_k + \mu d_k \mathbf{x}_k^*. \quad (7)$$

By assuming that the weight vectors are initialized to be zeros, i.e., $\mathbf{g}_0 = \mathbf{h}_0 = \mathbf{0}$, we next investigate the evolutions of both $\mathbf{g}_k$ and $\mathbf{h}_k$ on a step-by-step basis. For simplicity, we discuss in detail the evolution of $\mathbf{g}_k$ and directly state the corresponding result for $\mathbf{h}_k$, which can be calculated analogously. According to (6), we have

$$\mathbf{g}_1 = \left(\mathbf{I} - \mu \mathbf{x}_0 \mathbf{x}_0^H\right)\mathbf{g}_0 - \mu \mathbf{x}_0 \mathbf{x}_0^T \mathbf{h}_0 + \mu d_0 \mathbf{x}_0 = \mu d_0 \mathbf{x}_0. \quad (8)$$

In the next stage,

$$\begin{aligned}\mathbf{g}_2 &= \left(\mathbf{I} - \mu \mathbf{x}_1 \mathbf{x}_1^H\right)\mathbf{g}_1 - \mu \mathbf{x}_1 \mathbf{x}_1^T \mathbf{h}_1 + \mu d_1 \mathbf{x}_1\\ &= \mu\left(d_0 \mathbf{x}_0 + d_1 \mathbf{x}_1\right) - \mu^2 \mathbf{x}_1\left(\mathbf{x}_1^H \mathbf{x}_0 + \mathbf{x}_1^T \mathbf{x}_0^*\right) d_0, \quad (9)\end{aligned}$$

where the inner products $\mathbf{x}_1^H \mathbf{x}_0$ and $\mathbf{x}_1^T \mathbf{x}_0^*$ can be evaluated as

$$\mathbf{x}_1^H \mathbf{x}_0 = \frac{1}{N}\sum_{l=0}^{N-1} e^{-i\frac{2\pi}{N}l} = 0, \quad \mathbf{x}_1^T \mathbf{x}_0^* = \frac{1}{N}\sum_{l=0}^{N-1} e^{i\frac{2\pi}{N}l} = 0. \quad (10)$$

Then, equation (9) reduces to

$$\mathbf{g}_2 = \mu\left(d_0 \mathbf{x}_0 + d_1 \mathbf{x}_1\right). \quad (11)$$

In a similar way, from (7), we have

$$\mathbf{h}_1 = \mu d_0 \mathbf{x}_0^*, \ \mathbf{h}_2 = \mu\left(d_0 \mathbf{x}_0^* + d_1 \mathbf{x}_1^*\right). \quad (12)$$

Following the same procedure, for the time instant k,

$$\mathbf{g}_k = \mu \sum_{l=0}^{k-1} d_l \mathbf{x}_l, \quad \mathbf{h}_k = \mu \sum_{l=0}^{k-1} d_l \mathbf{x}_l^*, \quad k = 1, \ldots, N, \quad (13)$$

so that, when $k = N$, we have

$$\begin{aligned}\mathbf{g}_N &= \mu \sum_{l=0}^{N-1} d_l \mathbf{x}_l\\ &= \frac{\mu}{\sqrt{N}} \sum_{l=0}^{N-1} d_l \left[1, e^{i2\pi l/N}, \ldots, e^{i2\pi(N-1)l/N}\right]^T\\ &= \frac{\mu}{\sqrt{N}}\left[\sum_{l=0}^{N-1} d_l, \sum_{l=0}^{N-1} d_l e^{i2\pi l/N}, \ldots, \sum_{l=0}^{N-1} d_l e^{i2\pi(N-1)l/N}\right]^T, \quad (14)\end{aligned}$$

$$\begin{aligned}\mathbf{h}_N &= \mu \sum_{l=0}^{N-1} d_l \mathbf{x}_l^*\\ &= \frac{\mu}{\sqrt{N}}\left[\sum_{l=0}^{N-1} d_l, \sum_{l=0}^{N-1} d_l e^{-i2\pi l/N}, \ldots, \sum_{l=0}^{N-1} d_l e^{-i2\pi(N-1)l/N}\right]^T. \quad (15)\end{aligned}$$

From (14) and (15), observe that except for the scale factor, μ, the elements of $\mathbf{g}_N$ and $\mathbf{h}_N$ respectively comprise the IDFT and DFT coefficients of d_k, over the time window of corresponding samples from $k = 0$ to $k = N-1$. However, we should note that formulae in (13) are derived based on the orthogonality among $\{\mathbf{x}_0, \mathbf{x}_1, \ldots, \mathbf{x}_{N-1}\}$, and hence, they are valid only when $1 \leq k \leq N$. Beyond this range, we need new formulae since, for instance, $\mathbf{x}_N$ becomes identical to $\mathbf{x}_0$, and they are not orthogonal, i.e., $\mathbf{x}_N^H\mathbf{x}_0 = \mathbf{x}_0^H\mathbf{x}_0 \neq \mathbf{0}$. To address this issue, once again from (6), we have

$$\begin{aligned}\mathbf{g}_{N+1} &= \left(\mathbf{I}-\mu\mathbf{x}_N\mathbf{x}_N^H\right)\mathbf{g}_N-\mu\mathbf{x}_N\mathbf{x}_N^T\mathbf{h}_N+\mu d_N\mathbf{x}_N\\ &= \mu\sum_{l=0}^{N} d_l\mathbf{x}_l-\mu^2\mathbf{x}_N\left(\mathbf{x}_N^H\sum_{l=0}^{N-1} d_l\mathbf{x}_l\right)\\ &\quad -\mu^2\mathbf{x}_N\left(\mathbf{x}_N^T\sum_{l=0}^{N-1} d_l\mathbf{x}_l^*\right),\end{aligned} \tag{16}$$

in which, the product $\mathbf{x}_N\left(\mathbf{x}_N^H\sum_{l=0}^{N-1} d_l\mathbf{x}_l\right)$ can be decomposed as

$$\mathbf{x}_N\left(\mathbf{x}_N^H\sum_{l=0}^{N-1} d_l\mathbf{x}_l\right) = \mathbf{x}_N\left(\mathbf{x}_N^H\left[d_0\mathbf{x}_0+\sum_{l=1}^{N-1} d_l\mathbf{x}_l\right]\right). \tag{17}$$

Furthermore,

$$\mathbf{x}_N^H d_0\mathbf{x}_0 = d_0\mathbf{x}_0^H\mathbf{x}_0 = d_0, \tag{18}$$

$$\mathbf{x}_N^H\sum_{l=1}^{N-1} d_l\mathbf{x}_l = \mathbf{x}_0^H\sum_{l=1}^{N-1} d_l\mathbf{x}_l = 0. \tag{19}$$

Similarly,

$$\mathbf{x}_N\left(\mathbf{x}_N^T\sum_{l=0}^{N-1} d_l\mathbf{x}_l^*\right)=\mathbf{x}_N\left(\mathbf{x}_N^T\left[d_0\mathbf{x}_0^*+\sum_{l=1}^{N-1} d_l\mathbf{x}_l^*\right]\right)=\mathbf{x}_N d_0. \tag{20}$$

Substituting (17)-(20) back into (16) simplifies the update process of $\mathbf{g}_{N+1}$, to yield

$$\mathbf{g}_{N+1}=\mu\sum_{l=0}^{N} d_l\mathbf{x}_l-2\mu^2\mathbf{x}_N d_0=\mu\sum_{l=1}^{N} d_l\mathbf{x}_l+\mu(1-2\mu)\mathbf{x}_0 d_0. \tag{21}$$

In the next stage,

$$\begin{aligned}\mathbf{g}_{N+2} &= \mu\sum_{l=0}^{N+1} d_l\mathbf{x}_l-2\mu^2\mathbf{x}_{N+1}d_1-2\mu^2\mathbf{x}_N d_0\\ &= \mu\sum_{l=2}^{N+1} d_l\mathbf{x}_l+\mu(1-2\mu)(\mathbf{x}_1 d_1+\mathbf{x}_0 d_0).\end{aligned} \tag{22}$$

In the same spirit, from (7), we have

$$\mathbf{h}_{N+1} = \mu\sum_{l=1}^{N} d_l\mathbf{x}_l^*+\mu(1-2\mu)\mathbf{x}_0^* d_0, \tag{23}$$

$$\mathbf{h}_{N+2} = \mu\sum_{l=2}^{N+1} d_l\mathbf{x}_l^*+\mu(1-2\mu)(\mathbf{x}_1^* d_1+\mathbf{x}_0^* d_0). \tag{24}$$

The results in (21)-(24) can now be generalized as the time evolves (until $k = 2N$), so that we arrive at

$$\begin{aligned}\mathbf{g}_k &= \mu\sum_{l=k-N}^{k-1} d_l\mathbf{x}_l+\mu(1-2\mu)\sum_{l=0}^{k-N-1} d_l\mathbf{x}_l,\\ \mathbf{h}_k &= \mu\sum_{l=k-N}^{k-1} d_l\mathbf{x}_l^*+\mu(1-2\mu)\sum_{l=0}^{k-N-1} d_l\mathbf{x}_l^*, \quad k=N+1,\dots,2N.\end{aligned} \tag{25}$$

After some algebraic manipulations in the same spirit, the general expressions for $\mathbf{g}_k$ and $\mathbf{h}_k$, which are applicable over all $k \geq 1$, now become

$$\begin{aligned}\mathbf{g}_k &= \mu\sum_{l=k-N}^{k-1} d_l\mathbf{x}_l+\mu(1-2\mu)\sum_{l=k-2N}^{k-N-1} d_l\mathbf{x}_l\\ &\quad +\mu(1-2\mu)^2\sum_{l=k-3N}^{k-2N-1} d_l\mathbf{x}_l+\cdots,\end{aligned} \tag{26}$$

$$\begin{aligned}\mathbf{h}_k &= \mu\sum_{l=k-N}^{k-1} d_l\mathbf{x}_l^*+\mu(1-2\mu)\sum_{l=k-2N}^{k-N-1} d_l\mathbf{x}_l^*\\ &\quad +\mu(1-2\mu)^2\sum_{l=k-3N}^{k-2N-1} d_l\mathbf{x}_l^*+\cdots.\end{aligned} \tag{27}$$

In both the above equations, the allowable range of the index l differs in each summation operation, and is governed by the respective upper and lower limits. However, note that the valid terms are those with $l \geq 0$. If we set $\mu = 1/2$ and let k be multiples of N, i.e., $k = \tau N$ where τ is a positive integer, the weight update processes of $\mathbf{g}_k$ and $\mathbf{h}_k$ become

$$\begin{aligned}\mathbf{g}_{\tau N} &= \mu\sum_{l=\tau N-N}^{\tau N-1} d_l\mathbf{x}_l = \frac{1}{2\sqrt{N}}\Bigg[\sum_{l=\tau N-N}^{\tau N-1} d_l, \sum_{l=\tau N-N}^{\tau N-1} d_l e^{i2\pi l/N},\\ &\qquad \dots, \sum_{l=\tau N-N}^{\tau N-1} d_l e^{i2\pi(N-1)l/N}\Bigg]^T,\end{aligned} \tag{28}$$

$$\begin{aligned}\mathbf{h}_{\tau N} &= \mu\sum_{l=\tau N-N}^{\tau N-1} d_l\mathbf{x}_l^* = \frac{1}{2\sqrt{N}}\Bigg[\sum_{l=\tau N-N}^{\tau N-1} d_l, \sum_{l=\tau N-N}^{\tau N-1} d_l e^{-i2\pi l/N},\\ &\qquad \dots, \sum_{l=\tau N-N}^{\tau N-1} d_l e^{-i2\pi(N-1)l/N}\Bigg]^T.\end{aligned} \tag{29}$$

Remark 1: The weight vectors $\mathbf{g}_{\tau N}$ in (28) and $\mathbf{h}_{\tau N}$ in (29) are proportional to the N-IDFT and N-DFT coefficients of the N previous samples of d_k when the time instant k is a multiple of N, indicating that with an appropriate choice of input vector and adaptation speed, the proposed WL-CLMS spectrum analyzer provides a unified means for the simultaneous calculation of N-sample block-based DFT and IDFT. Unlike the situation where the strictly linear CLMS is used to perform N-DFT or N-IDFT separately [1,10], the step-size μ of the WL-CLMS analyzer is half that of its CLMS counterpart. This is because WL-CLMS employs two weight vectors, the updates of which are coupled, and this doubles the weight dimensionality, as compared with the CLMS analyzer.

An illustration on using the proposed WL-CLMS spectrum analyzer to simultaneously implement block-based DFT and IDFT operations is provided in Fig. 2. The complex-valued signal to be Fourier analyzed, i.e., d_k, was generated as $d_k = 1+0.5i+0.8e^{i\pi k/2}+0.6e^{i5\pi/4}+n_k$, where n_k is a zero-mean complex-valued Gaussian noise, whose power was set to give the signal to noise ratio of 10 dB. Observe that after $N = 32$ iterations, the magnitudes of the standard weight coefficients $\mathbf{h}_k$ and the conjugate weights $\mathbf{g}_k$ of WL-CLMS were in exact accordance with those of block-based 32-DFT and 32-IDFT operations on d_k, respectively. This was also the case in the phase computation, which have not been provided due to the page limit.

3. ONLINE DFT AND IDFT COMPUTATION BY USING THE WL-CLMS SPECTRUM ANALYZER

It is of increasing interest to perform DFT and IDFT operations for streaming data, so as to provide online Fourier analysis [23, 24]. This recursive type of DFT and IDFT operations can be also simultaneously calculated by the proposed WL-CLMS spectrum analyzer which employs the adaptive mechanism displayed in Fig. 1. Similar to the analysis in [1], we define the online DFT and IDFT vectors of N data samples in a sliding window manner as

$$\mathrm{DFT}_k = \frac{1}{\sqrt{N}} \begin{bmatrix} \sum_{l=0}^{N-1} d_{k-(N-1)+l} \\ \sum_{l=0}^{N-1} d_{k-(N-1)+l} e^{-i2\pi l/N} \\ \vdots \\ \sum_{l=0}^{N-1} d_{k-(N-1)+l} e^{-i2\pi (N-1)l/N} \end{bmatrix}, \quad (30)$$

$$\mathrm{IDFT}_k = \frac{1}{\sqrt{N}} \begin{bmatrix} \sum_{l=0}^{N-1} d_{k-(N-1)+l} \\ \sum_{l=0}^{N-1} d_{k-(N-1)+l} e^{i2\pi l/N} \\ \vdots \\ \sum_{l=0}^{N-1} d_{k-(N-1)+l} e^{i2\pi (N-1)l/N} \end{bmatrix}. \quad (31)$$

By setting $\mu = 1/2$ and without loss of generality, upon changing the index l to $(l + k - N)$, equations (26) and (27) can be rewritten as

$$\mathbf{g}_k = \frac{1}{2\sqrt{N}} \begin{bmatrix} \sum_{l=0}^{N-1} d_{l+k-N} \\ e^{i2\pi k/N} \sum_{l=0}^{N-1} d_{l+k-N} e^{i2\pi l/N} \\ \vdots \\ e^{i2\pi (N-1)k/N} \sum_{l=0}^{N-1} d_{l+k-N} e^{i2\pi (N-1)l/N} \end{bmatrix}, \quad (32)$$

$$\mathbf{h}_k = \frac{1}{2\sqrt{N}} \begin{bmatrix} \sum_{l=0}^{N-1} d_{l+k-N} \\ e^{-i2\pi k/N} \sum_{l=0}^{N-1} d_{l+k-N} e^{-i2\pi l/N} \\ \vdots \\ e^{-i2\pi (N-1)k/N} \sum_{l=0}^{N-1} d_{l+k-N} e^{-i2\pi (N-1)l/N} \end{bmatrix}. \quad (33)$$

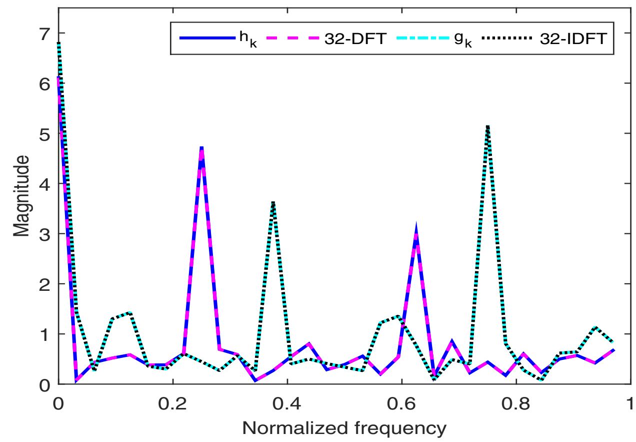

Fig. 2. Simulation results of the proposed WL-CLMS spectrum analyzer after $N = 32$ iterations.

Now, by comparing (30) and (33) and (31) and (32), the respective relations between the sliding DFT and IDFT operations and the WL-CLMS analyzer are obvious, and are given by

$$\mathrm{DFT}_{k-1} = 2\sqrt{N}\mathbf{X}_k \mathbf{h}_k, \quad (34)$$

$$\mathrm{IDFT}_{k-1} = 2\sqrt{N}\mathbf{X}_k^* \mathbf{g}_k, \quad (35)$$

where $\mathbf{X}_k$ is an $N \times N$ diagonal matrix, whose elements are drawn from the input vector $\mathbf{x}_k$ in (1). Therefore, by multiplying the weights $\mathbf{h}_k$ and $\mathbf{g}_k$ with the corresponding phasor components within $\mathbf{x}_k$ and $\mathbf{x}_k^*$, respectively, the proposed WL-CLMS spectrum analyzer provides a unified and simultaneous sliding window computation of DFT and IDFT operations over the N most recent samples of d_k from $(k - N)$ to $(k - 1)$.

4. CONCLUSIONS

Fundamental relations between the widely linear complex least mean square (WL-CLMS) adaptive filtering algorithm and both the discrete Fourier transform (DFT) and inverse DFT (IDFT) operations have been investigated. We have shown that with a choice of the speed of adaptation, $\mu = 1/2$, the standard and conjugate weight vectors within the proposed WL-CLMS spectrum analyzer are proportional to the block-based DFT and IDFT coefficients over N data samples after the filter converges. When the proposed WL-CLMS based spectrum analyzer operates in an online manner, the standard and conjugate weights are necessary to multiply with the corresponding phasors to provide sliding-window DFT and IDFT coefficients. Furthermore, the proposed widely linear spectrum analyzer can be straightforwardly extended to perform other complex-valued orthogonal transforms and their inverse transforms simultaneously, a subject of future work.

5. REFERENCES

[1] B. Widrow, P. Baudrenghien, M. Vetterli, and P. Titchener, "Fundamental relations between the LMS algorithm and the DFT," *IEEE Trans. Circuits Syst.*, vol. 34, no. 7, pp. 814–820, Jul. 1987.

[2] J. C. Liu and T. P. Lin, "LMS-based DHT analyser," *Electron. Lett.*, vol. 24, no. 8, pp. 483–485, Apr. 1988.

[3] J. Xi, "Relations between discrete Walsh transform and the adaptive LMS algorithm," in *Proc. Int. Conf. Circuits Syst.*, Jun. 1991, pp. 127–129.

[4] J. Xi and J. F. Chicharo, "Computing running discrete cosine/sine transforms based on the adaptive LMS algorithm," *IEEE Trans. Circuits Syst. Video Technol.*, vol. 8, no. 1, pp. 31–35, Feb. 1998.

[5] B. Liu and L. T. Bruton, "The two-dimensional complex LMS algorithm applied to the 2D DFT," *IEEE Trans. Circuits Syst. II*, vol. 40, no. 5, pp. 337–341, May. 1993.

[6] T. Ogunfunmi and M. Au, "2-D discrete orthogonal transforms by means of 2-D LMS adaptive algorithms," in *Proc. 28th Asilomar Conf. Signals, Syst. Comput. (ASILOMAR)*, Oct. 1994, pp. 1493–1496.

[7] M. T. Haweel and T. I. Haweel, "Adaptive LMS discrete 2-D orthogonal transforms," in *Proc. Jpn.-Egypt Conf. Electron., Commun. Comput. (JEC-ECC)*, Dec. 2013, pp. 194–197.

[8] F. Beaufays and B. Widrow, "On the advantages of the LMS spectrum analyzer over nonadaptive implementations of the sliding-DFT," *IEEE Trans. Circuits Syst. I*, vol. 42, no. 4, pp. 218–220, Apr. 1995.

[9] W. Li, "Fourier analysis using adaptive AFT," in *Proc. IEEE Int. Conf. Acoust., Speech, Signal Process. (ICASSP)*, Apr. 1990, pp. 1523–1526.

[10] S. S. Wang, "LMS algorithm and discrete orthogonal transforms," *IEEE Trans. Circuits Syst.*, vol. 38, no. 8, pp. 949–951, Aug. 1991.

[11] B. Scalzo Dees, S. C. Douglas, and D. P. Mandic, "Complementary complex-valued spectrum for real-valued data: Real time estimation of the panorama through circularity-preserving DFT," in *Proc. IEEE Int. Conf. Acoust., Speech, Signal Process. (ICASSP)*, 2018, pp. 3999–4003.

[12] A. H. Sayed, *Fundamentals of Adaptive Filtering*, New York: Wiley, 2003.

[13] P. J. Schreier and L. L. Scharf, "Second-order analysis of improper complex random vectors and process," *IEEE Trans. Signal Process.*, vol. 51, no. 3, pp. 714–725, Mar. 2003.

[14] S. Javidi, M. Pedzisz, S. L. Goh, and D. P. Mandic, "The augmented complex least mean square algorithm with application to adaptive prediction problems," in *Proc. 1st IARP Workshop on Cognitive Information Processing (CIP)*, 2008, pp. 54–57.

[15] D. P. Mandic and S. L. Goh, *Complex Valued Nonlinear Adaptive Filters: Noncircularity, Widely Linear and Neural Models*, New York: Wiley, 2009.

[16] P. J. Schreier and L. L. Scharf, *Statistical Signal Processing of Complex-Valued Data: The Theory of Improper and Noncircular Signals*, Cambridge, U.K.: Cambridge University Press, 2010.

[17] B. Picinbono and P. Chevalier, "Widely linear estimation with complex data," *IEEE Trans. Signal Process.*, vol. 43, no. 8, pp. 2030–2033, Aug. 1995.

[18] L. Anttila, M. Valkama, and M. Renfors, "Circularity-based I/Q imbalance compensation in wideband direct-conversion receivers," *IEEE Trans. Veh. Technol.*, vol. 57, no. 4, pp. 2099–2113, Jul. 2008.

[19] D. P. Mandic, S. Javidi, S. L. Goh, A. Kuh, and K. Aihara, "Complex-valued prediction of wind profile using augmented complex statistics," *Renewable Energy*, vol. 34, pp. 196–201, 2009.

[20] Y. Xia, S. C. Douglas, and D. P. Mandic, "Adaptive frequency estimation in smart grid applications: Exploiting noncircularity and widely linear adaptive estimators," *IEEE Signal Process. Mag.*, vol. 29, no. 5, pp. 44–54, Sep. 2012.

[21] Z. Li, Y. Xia, W. Pei, K. Wang, and D. P. Mandic, "An augmented nonlinear LMS for digital self-interference cancellation in full-duplex direct-conversion transceivers," *IEEE Trans. Signal Process.*, vol. 66, no. 15, pp. 4065–4078, Aug. 2018.

[22] Y. Xia and D. P. Mandic, "Augmented performance bounds on strictly linear and widely linear estimators with complex data," *IEEE Trans. Signal Process.*, vol. 66, no. 2, pp. 507–514, Jan. 2018.

[23] C. M. Orallo, I. Carugati, S. Maestri, P. G. Donato, D. Carrica, and M. Benedetti, "Harmonics measurement with a modulated sliding discrete Fourier transform algorithm," *IEEE Trans. Instrum. Meas.*, vol. 63, no. 4, pp. 781–793, Nov. 2013.

[24] C. Shitole and P. Sumathi, "Sliding DFT-based vibration mode estimator for single-link flexible manipulator," *IEEE/ASME Trans. Mechatronics*, vol. 20, no. 6, pp. 3249–3256, Dec. 2015.